Design of an Optimal Low Cost Miniaturized Piezo-electric Device for Energy Harvesting from Human Motion

Maurine N. Andanje, Ahmed M.R. Fath Elbab and Bernard W. Ikua

Abstract—Energy harvesters collect and convert energy available in the environment into useful electrical power to satisfy the power requirements of autonomous systems. Development of a low-cost miniaturized device that can harvest energy from non-traditional sources is still a very attractive point of research. Such a device is essential for a wide variety of applications such as self-powered wireless sensors and biomedical implants in which energy source is needed.

This paper presents a detailed design of a miniaturized energy harvesting device that can harvest human motion energy of low frequency and wide bandwidth. Based on the concept of the 2-DOF vibration system, the optimal parameters; namely, the proper masses and spring constants for maximizing the power output, are selected to harvest energy at low frequency of 1-10 Hz and wide bandwidth of $\pm$ 20% of the mean frequency, which matches the human motion. The energy harvester is then subjected to harmonic accelerations of between 0.4g and 1g which represents the acceleration of the human motion [1]. A finite element model is developed in COMSOL to investigate the system performance with the selected parameters. Then, experimental work is carried out to validate the design methodology with the selected parameters and investigate the system performance. By varying the normalized frequency and redesigning the system parameters, the best ratio that gives the highest power output is determined.

The designed energy harvester prototype is expected to generate power of microwatts to milliwatt level between the system's two resonant frequencies. This amount of power is sufficient enough to provide additional power for wearable devices such as an activity monitor that is operated at microwatts power level hence extending the battery life.

Keywords—Energy Harvesting; Two Degree of freedom; PVDF, power conditioning circuit

I. INTRODUCTION

WITH the development of low power electronics and energy harvesting technology, self-powered systems have become a research hotspot over the last decade. The main advantage of self-powered systems is that they require minimum maintenance which makes them to be deployed in large scale or previously inaccessible locations. Therefore, the target of energy harvesting is to power autonomous fit and forget electronic systems over their lifetime [2] .

Among the many energy sources, mechanical energy can be found in instances where thermal or photonic energy is not suitable, which makes extracting energy from mechanical energy an attractive approach for powering electronic systems. The source of mechanical energy can be a vibrating structure, a moving human body or air/water flow induced vibration. The frequency of the mechanical excitation depends on the source: less than 10Hz for human movements and typically over 30Hz for machinery vibrations [2].

The kinetic energy is transferred to a proof mass of the energy harvester, where several transduction techniques can be used to transform it to electrical energy such as piezoelectric, electromagnetic and electrostatic [3]. These devices are designed to match their natural resonant frequency with that of the energy source to maximize the power output. So, the possibility of using body motion to convert the kinetic energy to electrical energy is a solution that can be used to power wearable or implantable systems, such as self-powered wireless sensors and biomedical implants without limited lifespan and periodic replacement.

An energy harvester has normally three main components: the micro-generator which converts ambient environment energy into electrical energy, the voltage booster which pumps up and regulates the generated voltage and the storage element [3].

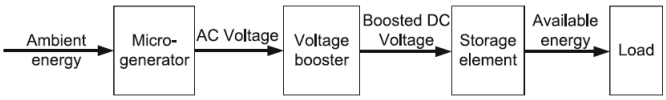

Fig. 1. Block diagram of an energy harvester [3]

A key challenge for vibration-based EH device is that it obtains the optimal power within a narrow frequency bandwidth near its resonant frequency. Away from the resonant frequency, the power generation drops dramatically and is too low to be utilized [4]. In fact, the frequencies of environmental vibration sources are relatively low (normally less than 200 Hz) and vary in a certain frequency range. As a result, energy harvesting mechanisms which can respond to low-frequency vibrations with wideband operation range or tunable resonant frequency are considered to be promising solutions.

Piezoelectric energy harvesters convert mechanical strain into voltage output, i.e., electric field across the piezoelectric layer, based on the piezoelectric effect. They have received much

M. N. Andanje, Department of Mechatronic Engineering, PAUISTI (e-mail: maureen.andanje@jkuat.ac.ke).

A. M.R. Fath Elbab, Department of Mechatronics and Robotics , EJUST (e-mail: ahmed.rashad@ejust.edu.eg).

B.K. Ikua, Department of Mechatronic Engineering, JKUAT (email:ikua$_b w@eng.jkuat.ac.ke$).

attention because of the advantages of simple configuration and high conversion efficiency [5]. The basic design idea is to enable maximum power extraction from the piezoelectric energy harvester by using the impedance matching circuit, i.e., to match the optimal load of the harvester to that of converter circuit [6].

II. LITERATURE REVIEW

Various types of piezoelectric energy harvesters have been studied which scavenge the wasted energy from human bodies and vibrating machines. Juil Park et al [4] proposed a new design for a cantilever-type piezoelectric energy harvester in which a free tip was excited by any rotary motion of mechanical devices. The experimental work done validated the simulation done in ANSYS using PVDF as the active material. The study verified that the design with the wider free tip was the optimized shape for the harvester subject to tip excitation. The new optimal design showed about 37% improvement in terms of charged energy when compared to the rectangular shape using the same amount of material.

Dhananjay Kumar et al [7], fabricated a piezoelectric energy harvester using six double sided piezoelectric diaphragms to generate regulated output of 5 Volts for load utilization. This boosted DC output was then used to charge a smart phone for 2.5 hours until full charge which was less than half the time required by the Li-Ion battery. Hua Yu [8] used an array of five cantilever beams and produced an output power of 66.75μW, with an optimal resistive load of 220 kΩ from 5 m/s^2 vibration acceleration at its resonant frequency of 234.5 Hz. The power conditioning circuit could provide a very promising complete power supply solution for wireless sensor node loads. Using an array of cantilevers, the researcher presented a significant improvement of output power and power density.

Isaku Kanno [9] compared the power generation performance of piezoelectric energy harvesters of PZT and KNN thin films deposited on stainless steel cantilevers. The output power as well as the electromechanical coupling factor of KNN-EHs were lower than those of the PZT-EHs due to large dielectric loss (tan) of the KNN thin films on stainless cantilevers. For this research, the optimization of the deposition condition of the KNN thin films on the stainless steel would improve the output performance.

Qijia Cheng et al [10] demonstrated devices to harvest energy from two kinds of human motions: joint rotation driven device with non-resonant system and hand-terminal driven device with low resonant frequency and broad bandwidth. An external vibration source was applied with a root mean square amplitude of 6.68 m/s^2 at 16 Hz .Voltage output of the joint rotation driven energy harvester was sinusoidal in shape with peak-to-peak value up to 10V. Voltage output of hand-terminal driven energy harvester could be as high as 40V peak-to-peak. The device was very sensitive to small vibration.

B Bayik et al [11] developed a multi-mode equivalent circuit model of a piezo-patch energy harvester integrated to a thin plate and coupled with a standard ACDC conversion circuit. Equivalent circuit parameters were obtained from the modal analysis solution of a distributed-parameter analytical model and from the finite-element numerical model of the harvester. From this work, the voltage output of the analytical model matched perfectly with Equivalent Circuit Model (simulated in SPICE) for different resistive load cases when parameters are identified from the analytical model. Their approach eliminates the mass loading and volumetric occupancy of cantilever attachments.

Mahmoud et al [12] designed a macro-scale 2-DOF energy harvester prototype based on the human motion frequency range and bandwidth. Harvester parameters were selected according to the concept of the vibration absorber to achieve two close resonance frequencies at 20% of the mean frequency of the frequency range 1-10 Hz. Simulation and experimental work were carried out to validate the design parameters and the system performance. By subjecting the harvester to harmonic accelerations within 1g the proposed device provided a power of at least 18μW in between the two close resonant frequencies. This work was able to achieve higher power per square of the mean frequency compared to previous research.

III. ENERGY HARVESTER DESIGN

A 2-DOF vibration system-based energy harvester is considered, as shown in figure 3. It consists of two masses and two springs; namely, the first mass (m_1) and the second mass (m_2), the first spring (k_1) and the second spring (k_2). The wide bandwidth of this 2-DOF system is attributed to the frequency range between the two amplitude peaks at resonances compared to that of the one peak for the single-DOF system.
The design flow of the energy harvester is as shown in Fig. 2:

A. Energy Harvester Mathematical Model

The dynamic model of this system under the base excitation force of $F = F_o sin\omega t$ is given as follows [12]:

$$\begin{bmatrix} m_1 & 0 \\ 0 & m_2 \end{bmatrix} \begin{bmatrix} \ddot{x_1} \\ \ddot{x_2} \end{bmatrix} + \begin{bmatrix} k_1 + k_2 & -k_2 \\ -k_2 & k_2 \end{bmatrix} \begin{bmatrix} x_1 \\ x_2 \end{bmatrix} = \begin{bmatrix} f_o sin\omega t \\ 0 \end{bmatrix}, \tag{1}$$

Where f_0 and ω are the amplitude and frequency of the exciting force, respectively x_1 and x_2 is the displacements of m_1 and m_2, respectively. The amplitudes X_1 and X_2 can be expressed as:

$$X_1 = \frac{(k_2 - m_2\omega^2) f_o}{(k_1 + k_2 - m_1\omega^2)(k_2 - m_2\omega^2) - k_2^2}, \tag{2}$$

$$X_2 = \frac{k_2 f_o}{(k_1 + k_2 - m_1\omega^2)(k_2 - m_2\omega^2) - k_2^2}, \tag{3}$$

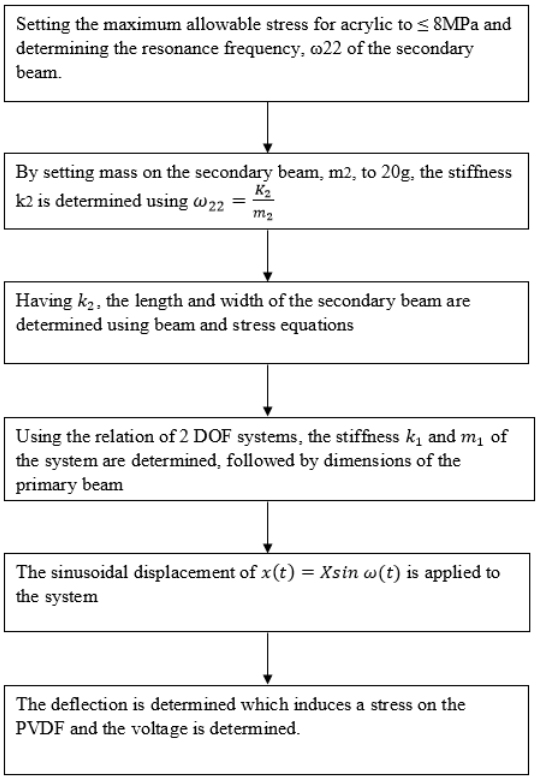

Fig. 2. Design Flow of the energy harvester

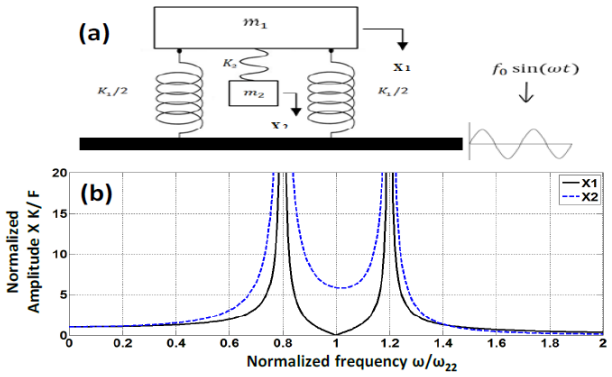

Fig. 3. (a) Schematic diagram of a vibration absorber; (b) Normalized amplitudes vs. normalized frequency [12]

It is evident from equation (2) that the amplitude X_1 of the main system mass becomes zero when the exciting frequency ω reaches the value of $\omega_{22} = \sqrt{k_2/m_2}$. At this condition, the amplitude of the second mass becomes $X_2 = -f_0/k_2$ as shown in Fig. 3.1 (b).
This is the condition for the second spring-mass system to work as a vibration absorber; suppressing the displacement of the first mass. This condition plays a critical role in the design, as it will be explained later. The maximum energy, which can be gained from the 2-DOF harvester system, is the amount of the dissipated energy by the absorber damping c_2.

Therefore, the output power (P) depends on the difference between the amplitudes of the two masses and the damping value (c_2) as follows [13]:

$$P = c_2\omega^2(X_2 - X_1)^2 \tag{4}$$

Where c_2 is the equivalent damping ratio due to transaction from mechanical to electrical energy. Satisfying the above condition achieves the following merits:

1) A large amplitude difference between the two masses over the targeted frequency range, which increases the resultant output power.
2) The continuity of the output signal due to existence of two close resonance peaks in the targeted bandwidth without compromising the power density (power/volume).
3) Keeping the first mass almost stationary at the most dominant frequency of the human motion during the daily activities. In case of using the piezoelectric material as transduction mechanism, this will avoid the voltage signal cancellation, due to the generation of a positive charge at the first spring k_1 and a negative charge at the second spring k_2 , when x_1 and x_2 are out of phase.

So, the system parameters (m_1, m_2, k_1, k_2) are selected to satisfy this condition. Also, low frequency (human motion) and wide bandwidth should be considered.

B. Energy Harvester Design Layout

The proposed device is designed as cut-out" beam as shown in Fig. (ref). It consists of two beams to act as the two springs k_1 and k_2 and two masses m_1 and m_2 which are located at the end of the two beams to act as a concentrated loads. The second beam k_2 is configured to get low value of spring stiffness. The proposed layout, cut-out beam design, is more compact than the conventional 2-DOF harvesters, because this design comprises one main cantilever and an inner secondary cantilever which reduces the total volume of the harvester.

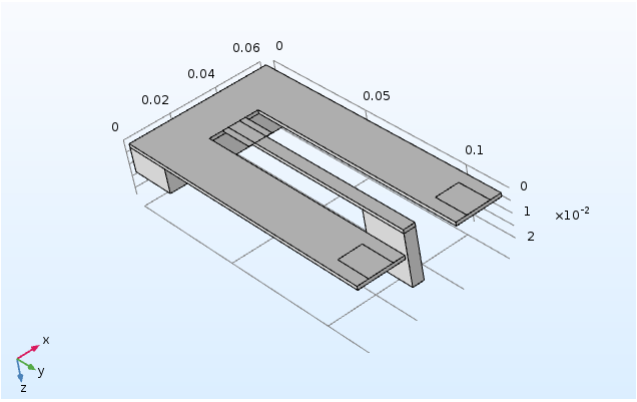

Fig. 4. Layout of the energy harvester

C. System Parameter Selection

In order to maximize on the generated power, the stress in the piezoelectric layer should be maximized. Poly methyl methacrylate(PMMA), also known as acrylic or acrylic glass

is used to design the harvester. It is preferred because of its moderate properties, easy handling and processing, and low cost. Although the tensile strength of acrylic sheets used is 69 MPa at room temperature, stress crazing can be caused by continuous loads below this value. For most applications, continuously imposed design loads should not exceed 10.4 MPa [14]. With this condition, the required mass m_2 which affect the stress induced in second beam k_2 and subsequently on the stress of piezoelectric layer is determined. The stress σ induced in the second beam k_2 can be calculated as:

$$\sigma = \frac{Fl_2Y}{I} \tag{5}$$

Where:

$$F = m_2 \times a \approx F = \frac{3EId}{l_2^3} \tag{6}$$

- F is the effective force due to acceleration of 1g, which is the most dominant acceleration of the human motion.
- Y = t_2/2 in which t_2 is the thickness of the beam
- I = Moment of inertia i.e. I = $b_2t_2^3/12$
- E = Young's modulus
- d = allowable deflection
- l_2 = length of the secondary beam
- b_2 = width of the secondary beam
- t_2 = thickness of the secondary beam

Substituting the moment of inertia:

$$F = \frac{E \times b_2 \times t_2^3 \times d}{4 \times l_2^3} \tag{7}$$

Substituting equation (7) into (5), the relation between the stress and thickness is given by:

$$\sigma = \frac{3 \times E \times t_2 \times d}{2 \times l_2^2} \tag{8}$$

Similarly, using the force equation (6) the stress can be represented as:

$$\sigma = \frac{m_2 \times a \times l_2 \times 6}{b_2 \times t_2^2} \tag{9}$$

In order to get a reasonable stiffness for the secondary beam, m_2 is set to 20g.

$$\omega_{22} = \sqrt{\frac{k_2}{m_2}} \tag{10}$$

Using equation (10) and at resonance when $\omega = \omega_{22} = 30$ rads/s, the value of k_2 = 18N/m.
Given the formular for the stiffness of a bending beam:

$$K = \frac{3EI}{L^3} \tag{11}$$

and

$$I = \frac{bt^3}{12} \tag{12}$$

An acrylic sheet with a thickness of 1.5 mm is used hence the length and width of the secondary beam is found to be: 90mm x 4.86mm.

Since the mean frequency of human motion is at 5Hz (30 rad/s), the bandwidth ratio is selected at $\pm$ 20% to match the human motion. Thus the two natural frequencies of the system are selected as ω_1^2 =24 rad/s and ω_2^2 =36 rad/s From the characteristic equations of the 2-DOF vibration system, the relationship between the two resonance frequencies and the system parameters (m_1, m_2, k_1, k_2) can be obtained as follows:

$$\omega_1^2 \times \omega_2^2 = \frac{k_1}{m_1} \times \frac{k_2}{m_2} \tag{13}$$

and

$$\omega_1^2 + \omega_2^2 = \frac{k_1}{m_1} + \frac{k_2}{m_2} + \frac{k_2}{m_1} \tag{14}$$

From equation (13) and (14), the primary beam will have a mass, m_1 of 126.3g and stiffness, k_1 of 104.7N/m. Using equation (11) and (12), the dimension of the primary beam with an acrylic sheet of thickness 1.5mm, is found to be 100mm x 38.8mm. The masses m_1 and m_2 are made from copper due to its high density of 8940 kg/m^3

The piezoelectric layer used is polyvinylidene fluoride (PVDF). This is a piezoelectric polymer which portrays favourable characteristics including; useful strain values, chemical inertness, robustness, relative ease of manufacture and low cost of raw materials. PVDF is also flexible, unlike ceramics, and therefore can be used in many applications where mechanical flexibility is required. Piezoelectric ceramics have the limitations of low yield strains, high density, brittleness and high costs of raw materials and manufacture. These are overcome by use of piezoelectric polymers [15].

When an input vibration applies acceleration to the beam structure, the effective mass converts the input acceleration into force. The relative displacement causes the PVDF strip to be tensed or compressed, which in turn induces a charge shift and accumulation due to the piezoelectric effect. Electrodes collect the generated charge and electrical damping results. The magnitude of the electric charge voltage is proportional to the stress induced by the relative displacement [8].

TABLE I
DIMENSIONS OF THE ENERGY HARVESTER

Parameter	Description	Value
L_d	Length of the device	135mm
W_d	Width of the device	105.8mm
l_1	Length of primary beam k_1	125mm
l_2	Length of secondary beam k_2	115mm
w_1	width of primary beam k_1	37.9mm
w_2	width of secondary beam k_2	10mm
t	thickness of the beam	1.5 mm
m_1	mass of primary beam k_1	126.3g
m_2	mass of secondary beam k_2	20g

IV. FINITE ELEMENT ANALYSIS

In this section, COMSOL software is used for creating a virtual testing setup for the proposed EH devices with the

calculated parameters. The springs k_1 and k_2 of the EH device are modelled from acrylic material with a Young's modulus of 3.2GPa. The proof masses m_1 and m_2 are modelled from Copper with a Young's Modulus of 117GPa. The dimensions of the EH device are as shown in table 1. Then, the boundary conditions are taken as:

1) The resonance frequency is set at 30rad/s with a bandwidth of $\pm$ 20%
2) The exciting frequency range is chosen to be between 1-10 Hz.
3) The exciting acceleration is taken to be 1g
4) The end of the primary beam is fixed
5) A base excitation force of $f = f_o sin\omega t$ is applied to the model.

A. Modal Analysis

A modal analysis is performed in COMSOL to determine the eigen frequencies and eigen modes of the energy harvester. Eigen frequencies or natural frequencies are certain discrete frequencies at which a system is prone to vibrate. When vibrating at a certain eigen frequency, the structure deforms into a corresponding shape, the eigen mode.

TABLE II
SIMULATION VALUES OF THE FIRST THREE NATURAL VALUES

Mode	Frequency Value
First Mode	4.0532 Hz
Second Mode	6.1103 Hz
Third Mode	19.85 Hz

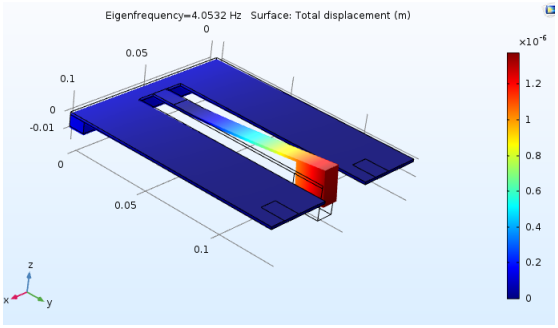

Fig. 5. First modal shape at 4.0532Hz

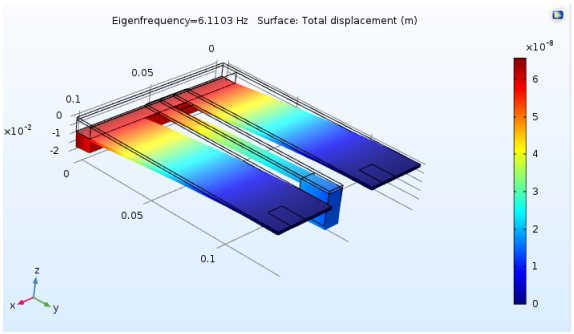

Fig. 6. Second modal shape at 6.1103 Hz

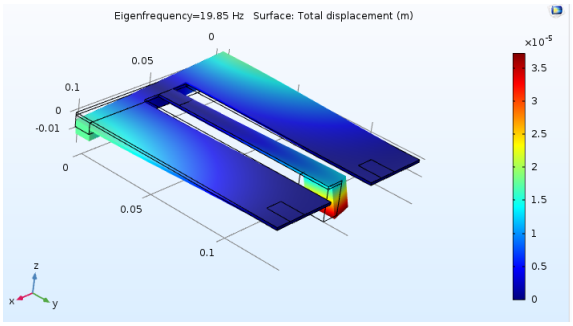

Fig. 7. Third modal shape at 19.85Hz

From figures 5 and 7 it can be seen that the two cantilevers are out of phase. In figure 6, the two cantilevers move in phase. The first two modes have natural frequencies that are below 10Hz which matches that of the human motion.

B. Stress Analysis

As expected, maximum stress is experienced at the joints of the cantilevers. This is where the piezoelectric strips are fixed so that they can have maximum stress applied on them for the deformation to occur and subsequently have electric charge emitted.

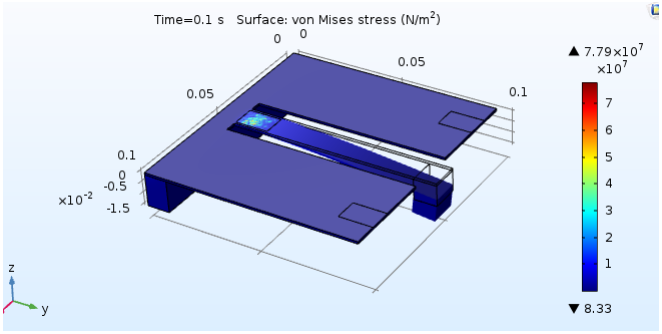

Fig. 8. Von Mises Stress (N/m^2) at 5Hz

In the simulation, a prescribed displacement of x(t)= Xsinωt is applied in the z direction of the energy harvester. The amplitude, X, is calculated to be 11 mm at an acceleration of 1g and frequency of 5Hz. Since this is the mean resonance frequency of the system, the deflection is only at the secondary beam and not the primary beam as expected from the design consideration of the shock absorber mode. From simulation results the maximum stress is 7.79 x 10^7 Pa.

C. Voltage generation and Power Calculation

Considering such piezoelectric cantilever operating in 31 mode, meaning the mechanical stress/strain is applied in the axial direction (1-direction) and electrical field/displacement generated in transverse direction (3-direction), the piezoelectric constitutive equation is described as [5]:

$$D_3 = \epsilon_{33} E_3 + d_{31}\sigma_1 \tag{15}$$

$$\xi_1 = s_{11}\sigma_1 + d_{31}E_3 \tag{16}$$

where ξ_1 and σ_1 are the axial mechanical strain and stress; E_3 and D_3 are the transverse electric field and electric displacement; s_{11}, ϵ_{33}, and d_{31} denote the axial elastic compliance at a constant electric field, the transverse dielectric coefficient measured at a constant stress, and the transverse axial piezoelectric constant.

According to Equation (15) and (16), the applied mechanical strain induces an electric displacement in the piezoelectric layer. Meanwhile, an electric field develops across the electrodes in the thickness direction and sends feedback to the mechanical domain thus affecting the mechanical strain. As the piezoelectric cantilever is connected to an external electric circuit and the load resistance is increased from zero to infinity, the system changes from short-circuit to open-circuit conditions. For the calculation of short-circuit current, it is assumed that E_3 = 0; while for the calculation of open-circuit voltage, it is assumed that D_3 = 0. The overall open-circuit voltage of each PVDF element related to the mass tip displacement is derived as [5]:

$$V_{oc} = -\frac{1}{1-k^2}\frac{d_{31}Yt_e}{\varepsilon_{33}l_b}3\frac{(l_b+l_m)t_b}{4l_b^2+9l_bl_m+6l_m^2}\delta_m \tag{17}$$

The average power delivered to the connected load Z_L is:

$$P_{rms} = \frac{1}{2}\frac{|V_{oc}|^2}{|Z_P+Z_L|^2}R_e\{Z_L\} \tag{18}$$

Where Z_L is the load impedance and Z_P is the impedance of the piezoelectric material. The maximum power occurs when the load impedance Z_L matches the complex conjugate of the PVDF element, i.e., Z_L = Z_P. If the connected load is purely real, i.e., Z_L = R_L, the maximum average power occurs when the load matches the impedance magnitude of the PVDF element, i.e., R_L = $|Z_P|$ and can be derived as [5]:

$$P_{rms} = \frac{1}{4}\frac{|V_{oc}|^2}{|Z_P|+R_e\{Z_P\}} \tag{19}$$

Figure 9 shows the equivalent electromechanical circuit of the energy harvester with the parameters modelled as follows [16]:

TABLE III
PVDF AND BEAM SPECIFICATIONS

Parameter	Description	Value
k	electromechanical coupling coefficient	14 %
d_{31}	Transverse Piezo Strain Constant	23 x $10^-12\frac{m/m}{V/m}$
Y	Young's Modulus of PVDF	4 x $10^-12\frac{m/m}{V/m}$
t_e	PVDF thickness k_1	28 μm
ϵ_{33}	Transverse dielectric coefficient	113 x $10^-12F/m$
l_b	Supporting beam length	as per design
t_b	Supporting beam thickness	as per design
l_m	length of mass	as per design
δ_m	tip displacement	as per design

- the mass is modelled by an inductor with inductance $L_m = m$
- the stiffness of the piezoelectric beam is represented by a capacitor with capacitance $C_m = 1/k$

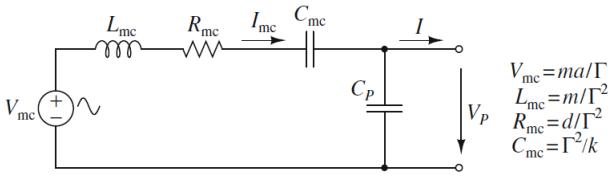

Fig. 9. Simplified electromechanical equivalent circuit of the piezoelectric harvester, where the coupling factor is considered in the lumped element parameters [16]

- the parasitic damping is modelled by a resistor with resistance $R_m = d$
- the alternating input force is modeled as a voltage source $V_m = m\ddot{y} = ma$
- V_p is the voltage across the piezoelectric terminals.
- C_p is the piezoelectric output capacitance

A circuit representation of a piezoelectric generator is shown in fig. 10 with a resistive load, R_L. C is the capacitance between two electrodes and R_s is the of the piezoelectric material. The voltage source, V_{OC}, is the open circuit voltage resulting from Eq. 15 when the electrical displacement is zero [3].

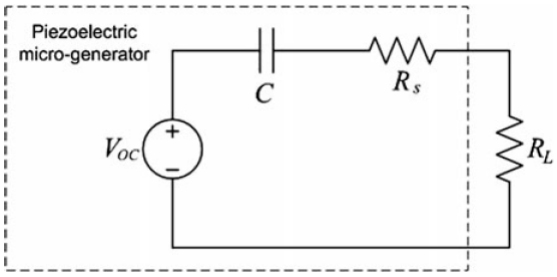

Fig. 10. Circuit representation of a piezoelectric generator [3]

where t is the thickness of the piezoelectric material, d_{31} is the piezoelectric strain coefficient and ε is the permittivity of the piezoelectric material.

D. Analytical Results

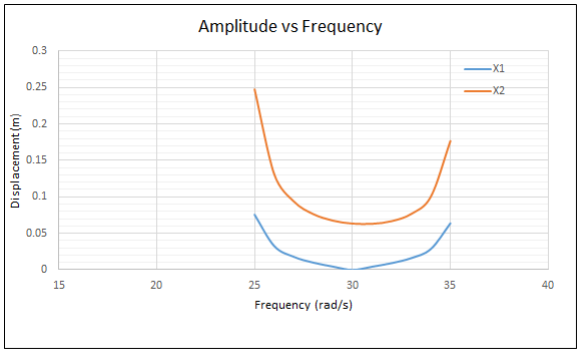

Fig. 11. Amplitudes X1 and X2 vs frequency

Figure 11 shows how the displacements of the two masses m_1 and m_2 compare. The proof mass on the secondary beam

is more displaced than the one on the primary beam. This is so because the design has used the concept of the shock absorber whereby at resonance, 30 rad/s, the displacement of the primary beam is minimized to zero. This is also illustrated in figure 12.

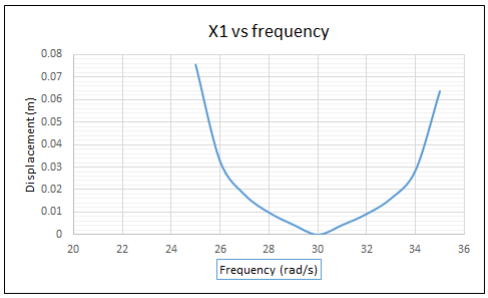

Fig. 12. Amplitude X1 vs Frequency

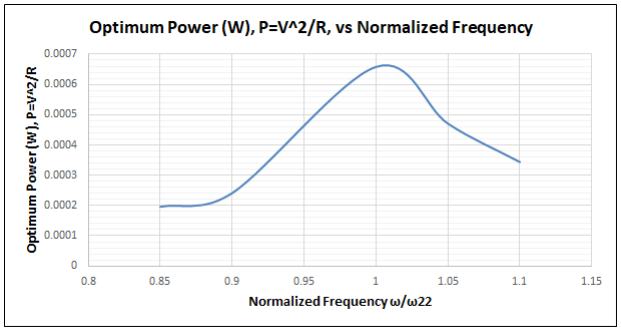

Fig. 13. Optimum Power vs Normalized frequency

Figure 13 shows that optimum power is generated at a frequency of 30 rad/s when the excitation frequency matches that of the energy harvester. Away from the resonance frequency, there is a reduction in the power generated. This is the case when the energy harvester is designed such that its resonance frequency matches that of the excitation source. However, if the design is different, then a different scenario is expected where the maximum energy might not always be at the point of resonance.

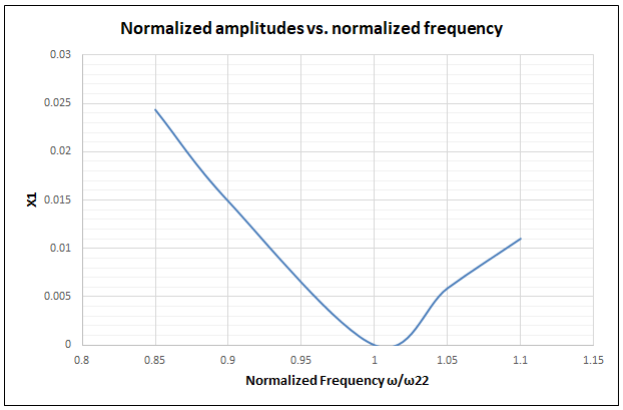

Fig. 14. Normalized amplitude vs Normalized frequency

The normalized amplitude will also have zero displacement for X_1 at the point where the normalized frequency is one, that is, the ratio of the excitation frequency to the resonance frequency of the energy harvester design is one. Away from this point, the amplitude of the primary beam will increase. Further work in this research will show how the other normalized frequency points will be utilized in energy harvesting to optimize on the power that can be generated on a 2 DOF system.

V. Conclusion

In this paper, a piezoelectric energy generator with power conditioning circuit is proposed. A complete design flow analyzing the architecture and parameters of the energy harvester using the FEM is established. Based on the simulation results, a 2 DOF cantilever system with copper proof masses is designed and fabricated. Analytical results show that the proposed energy harvester can produce a maximum output power of 40 μW with an optimal resistive load of 88 MΩ from 9.81 m/s^2 acceleration at its resonant frequency of 5 Hz with a bandwidth of $\pm$ 20%, which represents a significant improvement of output power.

Acknowledgment

The authors would like to thank PAUISTI and JICA for their financial support towards this research. Special thanks to EJUST for their invitation to utilize their Mechatronics lab for the fabrication and experimental testing of the designed prototypes.

References

[1] J. Yun, S. N. Patel, M. S. Reynolds, and G. D. Abowd, "Design and performance of an optimal inertial power harvester for human-powered devices," *IEEE Transactions on Mobile Computing*, vol. 10, no. 5, pp. 669–683, 2011.

[2] D. Zhu, *Vibration Energy Harvesting : Machinery Vibration , Human Movement and Flow Induced Vibration*. No. Viv, 2008.

[3] K. T. J and L. Wang, *Energy Harvester Systems Principles, Modeling and Applications*. 2011.

[4] J. Park, S. Lee, and B. M. Kwak, "Design optimization of piezoelectric energy harvester subject to tip excitation ," *Journal of Mechanical Science and Technology*, vol. 26, no. 1, pp. 137–143, 2012.

[5] H. Liu, C. J. Tay, C. Quan, T. Kobayashi, and C. Lee, "Piezoelectric MEMS energy harvester for low-frequency vibrations with wideband operation range and steadily increased output power," *Journal of Microelectromechanical Systems*, vol. 20, no. 5, pp. 1131–1142, 2011.

[6] S. Priya, H.-c. Song, Y. Zhou, R. Varghese, and A. Chopra, "A Review on Piezoelectric Energy Harvesting : Materials , Methods , and Circuits," vol. 4, no. 1, pp. 3–39, 2017.

[7] D. Kumar, P. Chaturvedi, and N. Jejurikar, "Piezoelectric energy harvester design and power conditioning," in *2014 IEEE Students' Conference on Electrical, Electronics and Computer Science*, no. March, pp. 1–6, 2014.

[8] H. Yu, J. Zhou, L. Deng, and Z. Wen, "A Vibration-Based MEMS Piezoelectric Energy Harvester and Power Conditioning Circuit," *Journal of Sensor Technology*, vol. 14, no. ISSN 1424-8220, pp. 3323–3341, 2014.

[9] I. Kanno, "Piezoelectric MEMS for energy harvesting," *Journal of Physics: Conference Series*, vol. 660, no. 1, 2015.

[10] Q. Cheng, Z. Peng, and J. Lin, "Energy Harvesting from Human Motion for Wearable Devices," in *10th IEEE International Conference on Nano/Micro Engineered and Molecular Systems (IEEE-NEMS 2015)*, pp. 409–412, 2015.

[11] B. Bayik, A. Aghakhani, I. Basdogan, and A. Erturk, "Equivalent circuit modeling of a piezo-patch energy harvester on a thin plate with AC DC conversion," *Smart Materials and Structures*, vol. 25, no. 5, p. 0, 2016.

[12] M. M. Magdy, N. A. Mansour, A. M. El-Bab, and S. F. Assala, "Human motion spectrum-based 2-DOF energy harvesting device: Design methodology and experimental validation," *Procedia Engineering*, vol. 87, pp. 1218–1221, 2014.

[13] X. Tang and L. Zuo, "Enhanced vibration energy harvesting using dual-mass systems," *Journal of Sound and Vibration*, vol. 330, no. 21, pp. 5199–5209, 2011.
[14] Kaysons, "Physical Properties of Acrylic Sheets,"
[15] H. S. Kim, J.-h. Kim, and J. Kim, "A Review of Piezoelectric Energy Harvesting Based on Vibration," *INTERNATIONAL JOURNAL OF PRECISION ENGINEERING AND MANUFACTURING*, vol. 12, no. 6, pp. 1129–1141, 2011.
[16] T. &. M. Y. Hehn, *CMOS Circuits for Piezoelectric Energy Harvesters*. 2015.